JOURNAL OF PHYSICAL ORGANIC CHEMISTRY
J. Phys. Org. Chem. 2000; **13:** 388–394

Solid-state reactivity of the hydrazine–hydroquinone complex

Gerd Kaupp* and Jens Schmeyers

Organische Chemie I, Universität Oldenburg, Postfach 2503, D-26111 Oldenburg, Germany

Received 10 January 2000; accepted 4 April 2000

epoc ABSTRACT: The solid-state reactivities of the hydrazine–hydroquinone 1:1 complex and of hydrazine hydrochloride with solid aldehydes, ketones, carboxylic acids, thiohydantoin and 4-nitrophenyl isothiocyanate were investigated. Only the hydrazine complex provides quantitative additions, condensations, ring openings and ring closures. The solid-state mechanisms were investigated by atomic force microscopy (AFM) and the far-reaching anisotropic molecular movements are correlated with the crystal packing, both on the hydrazine complex surface and on the surface of two benzaldehydes. The hydrazine moves into the aldehyde crystals for chemical reaction without melting. Characteristic surface features are created by the common phase rebuilding and phase transformation on both the hydrazine-donating and -accepting crystals. Copyright © 2000 John Wiley & Sons, Ltd.
Additional material for this paper is available from the epoc website at http://www.wiley.com/epoc

KEYWORDS: solid hydrazine; solid-state reactivity; anisotropic molecular movements; atomic force microscopy; crystal packing; carbonyl compounds; sustainable

INTRODUCTION

Hydrazine is a versatile though poisonous reagent, and quantitative reactions in the solid state[1–3] will facilitate its use. Unfortunately, solid salts of hydrazine such as the monohydrochloride (m.p. 89 °C) are of low reactivity in solid–solid reactions. However, the easily accessible 1:1 complex of hydrazine with hydroquinone deserves a closer look, as Toda *et al.* were able to use it for the conversion of solid esters into hydrazides in good yields.[4] We therefore tried a number of quantitative reactions with solid anhydrous hydrazine and solid carbonyl compounds and studied the mechanism in order to unravel the reasons for the success of the quantitative additions, condensations, ring openings and ring closures that emerged and may be conducted 'waste-free'[3] if the host hydroquinone is properly recycled.

RESULTS AND DISCUSSION

Azines

The reaction of solid aldehydes or ketones **1** with the hydrazine–hydroquinone complex **2** in a 2:1 ratio provides quantitatively solid mixtures of the azines **3** and hydroquinone **4** when ball-milled at room temperature. The previous host **4** is easily extracted with water at room temperature and the extract is concentrated by evaporation for precipitation of **2** with aqueous hydrazine hydrate. The solid-state double condensation is quantitative and more effective than the reported solution reactions [**3a**, no data; **3b**, 94% (1 h, room temperature);[5] **3c**, 92% (1 h, room temperature);[6] **3d**, 91%[7]]. On the other hand, solid-state reactions of **1** with hydrazine monohydrochloride remain largely incomplete. All of the aldehydes **1a–c** underwent complete reaction with **2** in 1 h, whereas 4-nitroacetophenone required a longer milling time for complete reaction even though dry powders were obtained in all cases. The water of reaction was fully included by the product crystals, most likely by **4**. It has been shown that 2.0 mmol of **4** take up 4.0 mmol of water in the ball-mill to form a dry, crystalline complex at room temperature (G. Kaupp and J. Schmeyers, unpublished work).

AFM investigation

The solid-state mechanism was elucidated by atomic force microscopy (AFM) for the hydrogen-bridged **1a** and the non-bridged **1c** in order to assess the directions of molecular movements in view of the known fact that the hydrazine is exhaustively bridged in **2**.[4]

The AFM analyses of the reaction of hydrazine–

**Correspondence to:* G. Kaupp, Organische Chemie I, Universität Oldenburg, Postfach 2503, D-26111 Oldenburg, Germany.
E-mail: kaupp@kaupp.chemie.uni-oldenburg.de
Contract/grant sponsor: Fonds der Chemischen Industrie.
Contract/grant sponsor: Deutsche Forschungsgemeinschaft.

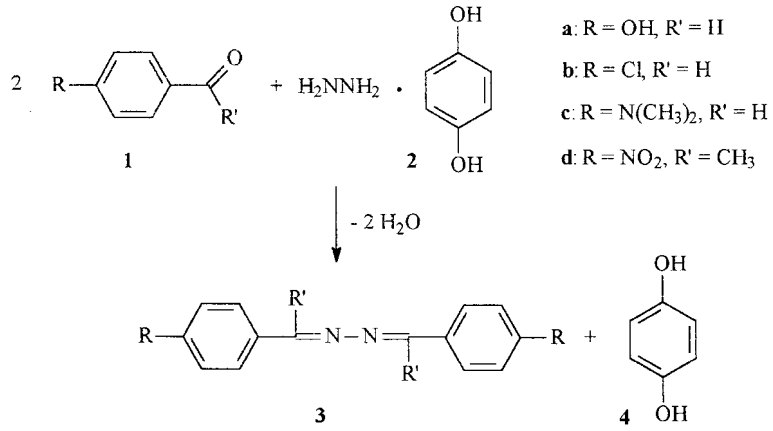

hydroquinone complex **2** and 4-hydroxybenzaldehyde (**1a**) is summarized in Figs 1 and 2. The reaction is rather slow. Almost no change of a smooth surface is observed in Fig. 1(b) at a 1 mm distance from the edge of the crystal **1a** that was placed on **2**. After a further 1 h the minute craters (<2 nm) were changed into skew floes that are about 10 nm in height at their steps in Fig. 1(c). The craters in Fig. 1(d) after 1 h at a 0.1 mm distance are typically 7 nm deep. Later, these became deeper (down to 50 nm) and additionally many small (20–30 nm) and some large hills (up to 100 nm) are present in Fig. 1(e). After 4 h, that site was too rough to be measured with the standard AFM but we recorded isolated volcano-like hills with heights of up to 220 nm at a 0.5 mm distance from the contact edge that are depicted in Fig. 1(f). Clearly, Fig. 1 indicates molecular movements above the (100)

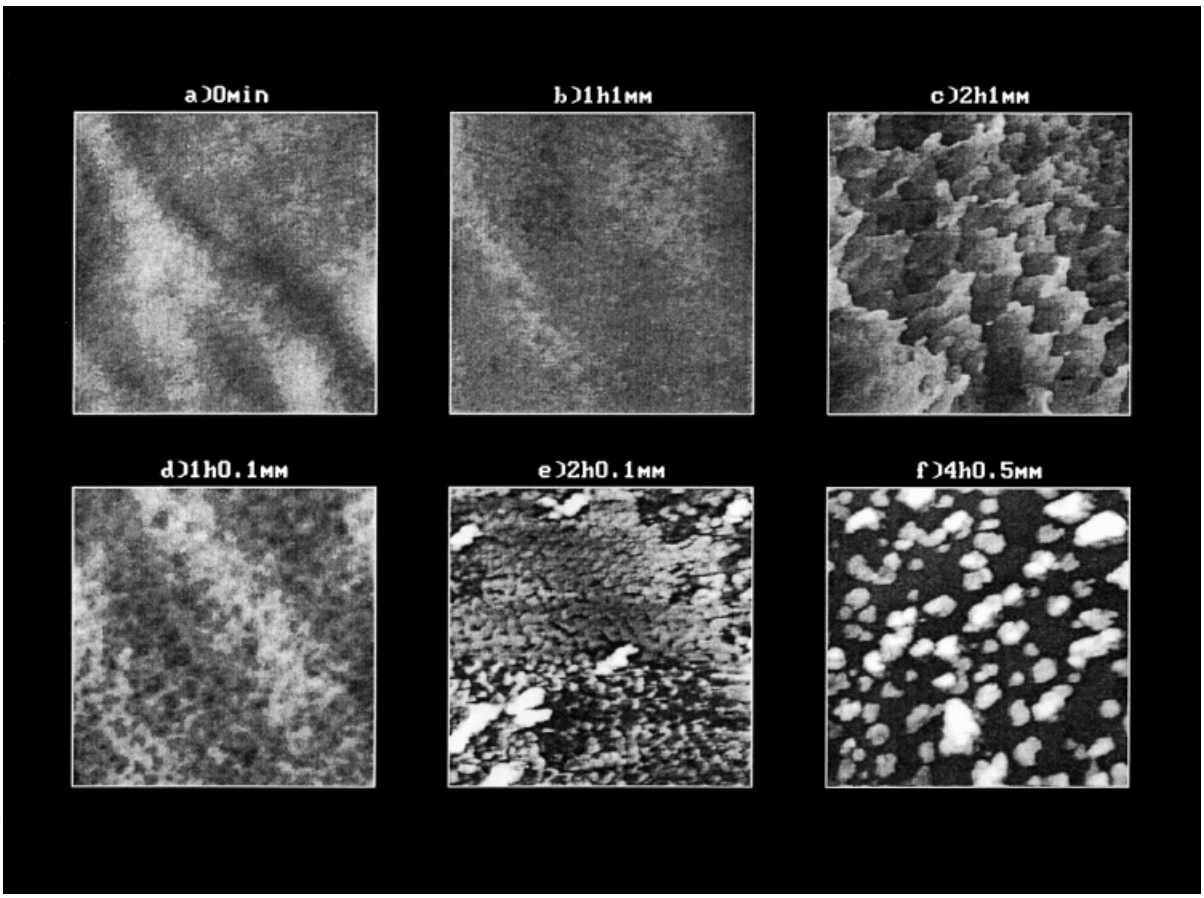

Figure 1. 10 μm AFM topographies of **2** (*C2/c;* plates) on (100) at 1, 0.5 and 0.1 mm distance from a crystal of **1a** that was placed on top of it. The reaction times are indicated. The *z*-scale is 100 nm in (a), (b), (c) and (d), 200 nm in (e) and 500 nm in (f). High-and low-resolution VRML images of (a)–(f) are available at the epoc website at http://www.wiley.com/epoc

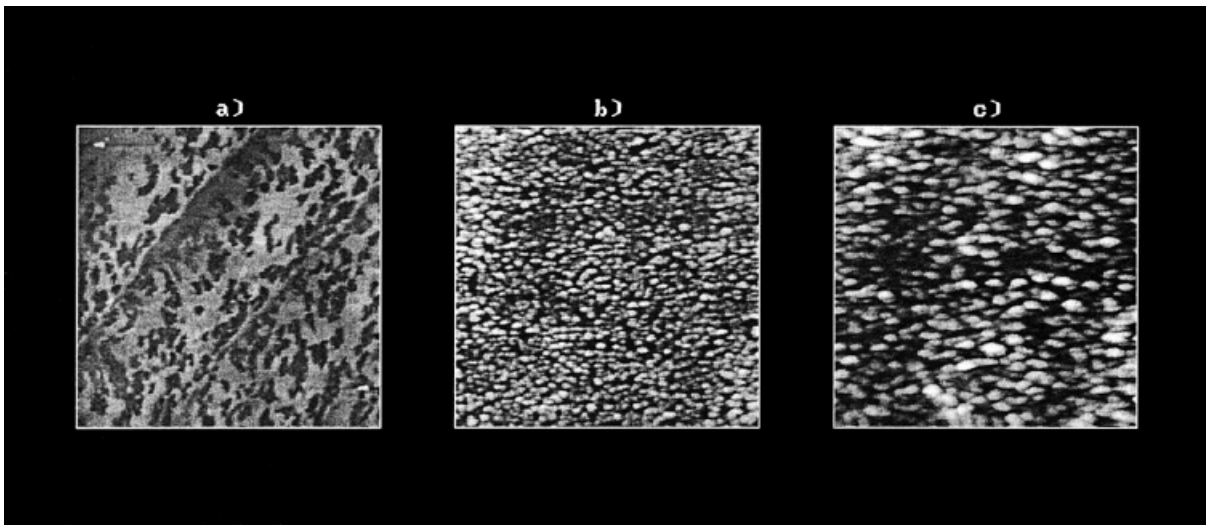

Figure 2. 10 μm AFM topographies of **1a** ($P2_1/c$; plates) on (010) at 0.1 mm distance from a crystal of **2** that was placed on top of it: (a) before placement; (b) after 5 min; (c) after 2 h. The *z*-scale is 100 nm in (a), 200 nm in (b) and 300 nm in (c). High-and low-resolution VRML images of (a)–(c) are available at the epoc website at http://www.wiley.com/epoc

face of **2** in two stages at a fairly close distance, which indicates phase rebuilding[8] [Fig. 1(e)] and finally phase transformation[8] [Fig. 1(f)] to give the host lattice [presumably as a water clathrate (G. Kaupp and J. Schmeyers, unpublished work)] on the surface. However, hydrazine moves away into the crystal of **1a**, which becomes yellow on formation of the solid azine **3a**. It was therefore also important to study the AFM features on a single crystal of **1a** with a crystal of **2** on it at a 0.1 mm distance where the product **3a** was formed. The result is shown in Figure 2.

A slighty corrugated initial surface (R_{ms} = 4.56 nm) created uniform 'egg trays' (416 craters and 663 volcanoes; R_{ms} = 14.73 nm) after 5 min of reaction. These had bottom to peak distances of about 80 nm [Fig. 2(b)] and they collapsed to give 157 and 191 broader and higher features after 2 h of reaction [Fig. 2(c)]. These features did not grow significantly until crystal disintegration occurred upon further reaction. Again, there was anisotropic molecular transport above the (010) face while leaving craters. No clear further direction of preference is discernable: the steep features in Fig. 2(c) are slightly distorted.

It was also important to study the reaction of crystals of non-hydrogen-bridged 4-dimethylaminobenzaldehyde (**1c**) on **2**. They withdrew the hydrazine molecules more rapidly from **2**. The initially corrugated surface of **2** in Fig. 3(a) (R_{ms} = 4.92 nm) formed craters (down to 300 nm deep) and volcanoes (up to 90 nm high) in 5 min at a 1 mm distance from the contact edge [Fig. 3(b)]. After 3 h the first signs of crystal disintegration were seen at that distance: the craters in Fig. 3(c) are down to 220 nm deep and start to form valleys. Some volcanoes are still present on the large floes. As in Fig. 1(e) and (f) there was molecular transport above the surface but it was more rapid and thus gave a different appearance of the features than in Fig. 1. The formation of the yellow azine **3c** is documented in Fig. 3(d)–(f) starting from a smooth surface (R_{ms} = 4.78) of **1c** with a crystal of **2** on it. Here flat covers [step height 50–150 nm in Fig. 3(e)] were rapidly formed (5 min) and in the next step huge islands appeared with heights of up to 970 nm, the slopes of which were frequently larger than 45°, so they appear somewhat broadened in the two 2-dimensional projection of Fig. 3(f). As expected, both phase rebuilding[8] and phase transformation[8] are totally different from the reaction of **1a** in Fig. 2.

Mechanistic discussion

The interpretation of the AFM results requires the consideration of the available crystal structures. The phase rebuilding on (010) of reacting **1a** has been described to give craters and volcanoes in the gas–solid reaction with methylamine.[2] Again, the reason is the steep packing of the molecules **1a**, half of them exposing their carbonyl function, the other half having it down in the crystal where it bridges to a phenolic OH group of the next layer. It is therefore not surprising to obtain the 'egg trays' [shown in Fig. 2(b), inasmuch as the molecules must move above the surface if their H-bonds are broken after reaction with hydrazine.[1,2] However, the second step, the phase transformation into the product lattice of **3a**, has nothing in common with the formation of extended craters in the referenced reaction.[2] In the present case we may admit some remaining guidance of the crystal packing of **1a** while the lattice of **3a** is formed in Fig. 2(c). The strongly different efficiency in the reaction of **1c** with **2** supports

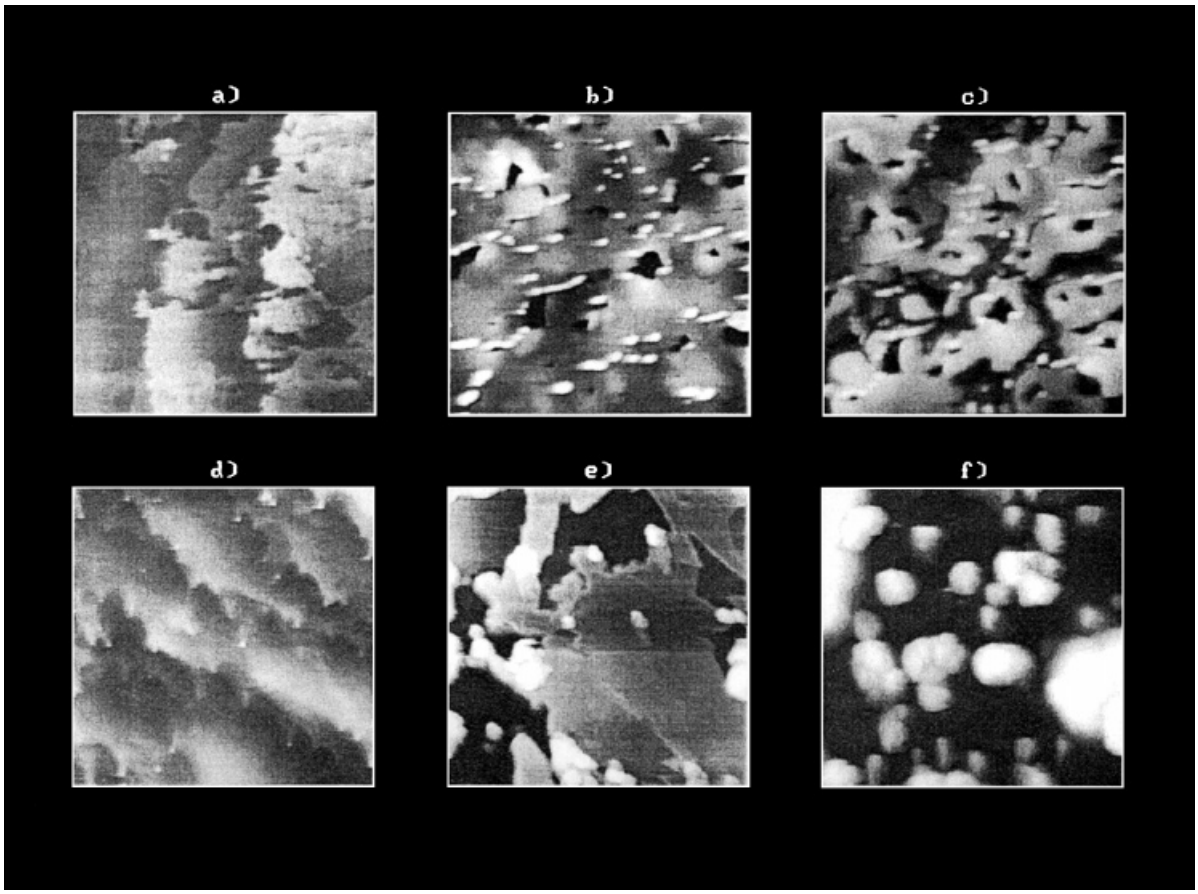

Figure 3. 10 μm AFM topographies of **2** on (100) with crystals of **1c** on top at a 1 mm distance: (a) fresh; (b) 5 min; (c) 3 h. 10 μm AFM topographies of **1c** (plates) on its main surface with crystals of **2** on top at a 0.1 mm distance: (d) fresh; (e) 5 min; (f) 43 min. The *z*-scales are 100 nm in (a) and (d), 200 nm in (b), 400 nm in (c) and (e) and 1400 nm in (f). High-and low-resolution VRML images of (a)–(f) are available at the epoc website at http://www.wiley.com/epoc

the view that hydrazine molecules move continuously from the complex through the contact points into the surface region of **1a** where they react to produce the intermediate hydrazone and finally the azine **3a** and two molecules of water that may move back to the host. Clearly, the condensation reaction spreads not only down into the bulk but also laterally, permitting its detection by AFM at remote sites. Vaporization of hydrazine along the surface of the reactant appears unlikely, as thermogravimetric analyses (TGA) did not show significant weight losses (at heating rates of 10 °C min^{-1}) below 80–100 °C. However, reactions of **2** at >100 °C[4] or even the reaction of **7** at 80 °C (see below) may be gas–solid reactions if the thermal exit of hydrazine gas from the lattice of **2** is fast enough. The crystal structure of **1c** is not known, but the flat covers[9] in Fig. 3(e) are certainly characteristic and the high and steep islands in Fig. 3(f) are probably the result of crystal characteristics of **3c** and do not require guidance by the initial lattice of **1c**.

The reactivity of the solid hydrazine–hydroquinone complex **2** was not foreseen, as the hydrazine is exhaustively hydrogen bridged: the hydrazine molecules in the bulk of the host lattice of **2** form six hydrogen bonds to six adjacent hydroxyl groups of six hydroquinone molecules (Fig. 4). The latter are bridged by hydrazine and form alternating layers. The NH···O distances are 3.131 and 3.161 Å and the OH···N distances are 2.732 Å. All free electron pairs and acidic hydrogens are involved in hydrogen bridges, which explains the high m.p. of 158 °C and stability of **2** (heating rate 10 °C min^{-1}; hydroquinone, m.p. 173–174 °C). It may be envisioned that the hydrazine molecules at the outer surfaces [e.g. at (100) at the top of Fig. 4] are released upon initial reaction and that a drain of hydrazine ensues in the layer parallel to (100). After higher dilution of the hydrazine in the outer layer, the layered hydroquinone molecules start to dangle and form hydrogen bonds with each other and most likely pick up the water of reaction in the condensations. By doing so, free space will be created for a drain from the next layer of hydrazine molecules, etc. Anyhow, we were not surprised that the solid-state reactions of **2** required longer milling times for complete reaction than the previous syntheses.[1,10] Similarly, Toda *et al.*'s acid hydrazide synthesis at 100–125 °C was not rapid (25

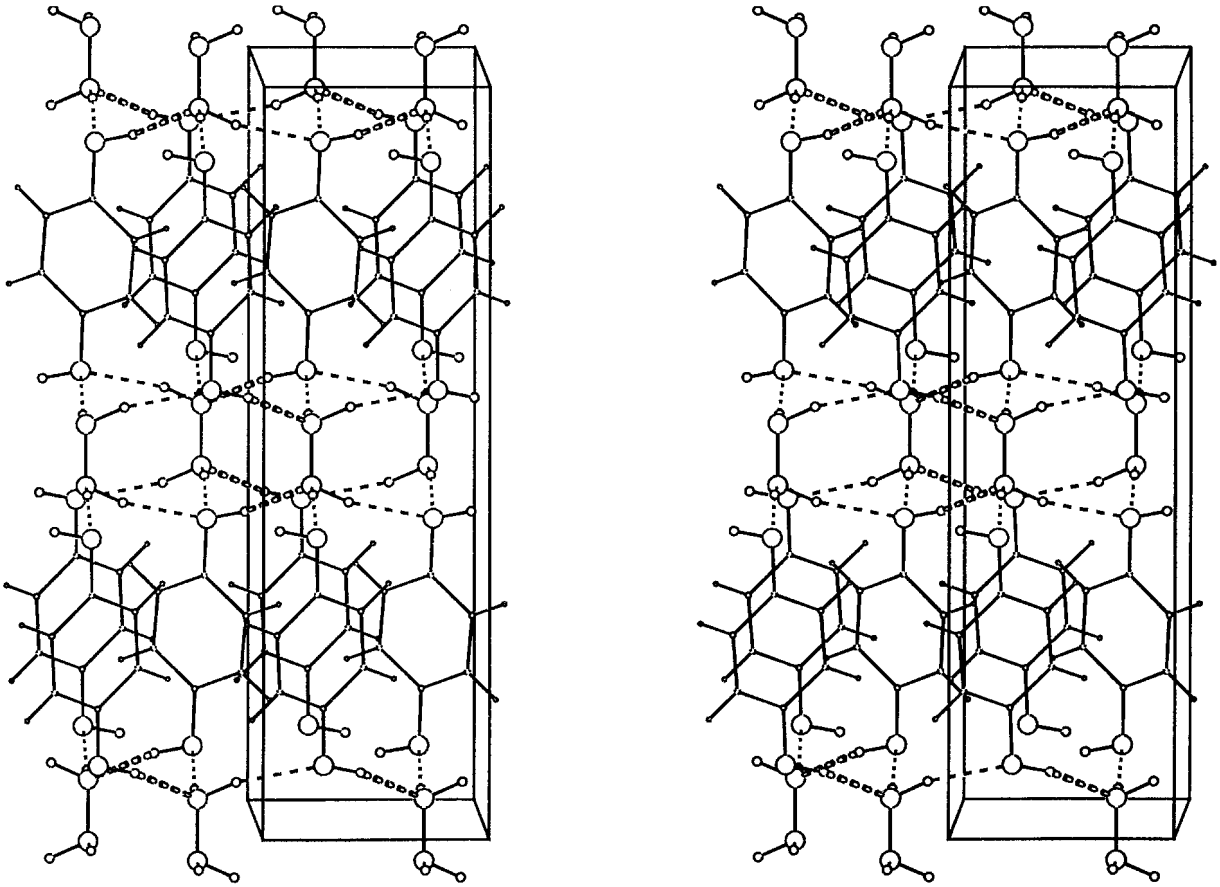

Figure 4. Stereoscopic view of the packing of the hydrazine–hydroquinone complex **2**[4] on (001) showing exhaustive hydrogen bridging. Large circles are N and O, small circles are H bound to N or O; thick hatches are OH···N and thin hatches NH···O hydrogen bridges. The top face is (100)

h).[4] Anyhow, the hydrogen bonds that are lost after exit of hydrazine may be replaced in a more and more distorted lattice of **2** that ends with the stable lattice of hydroquinone **4** or its water clathrate (G. Kaupp and J. Schmeyers, unpublished work). On the other hand, the low reactivity of solid hydrazine monohydrochloride is understandable from the crystal packing[11] (Fig. 5). Here both ionic and hydrogen bonds are present. The chloride anions are almost symmetrically located between two ammonium cation centers and the hydrogen bridges between NH_3^+ and NH_2 centers (N^+—H···N, 2.921 Å) build a three-dimensional network which is further stabilized by short N—H···Cl^- bridges (2.080, 2.242 and 2.347 Å) and does not allow the exit of the interlocked ions from the crystal because every hydrazinium cation is held in place by two strong ionic interactions and two strong hydrogen bonds. The energetics may be not so bad because the hydrochloride salts formed would experience ionic and hydrogen-bond interactions. However, there are kinetic obstacles that explain the failure of crystalline $N_2H_4 \cdot HCl$. At present, it cannot be foreseen if further salts of hydrazine might pack more favorably for exhibiting improved solid-state reactivity.

Applications

The mechanistic information was applied to the use of 'solid hydrazine' **2** for additions to the isothiocyanate **5** to give the thiosemicarbazide **6**, for ring opening of thiohydantoin **7** to give the thiourea hydrazide **8** and for cyclizations of **9** and **11** to give **10** and **12**. As, apparently, hydrazine is extracted from the host lattice by the reagents, we obtained quantitative yields of the highly functionalized products that are not available by milling the same starting crystals with hydrazine monohydrochloride at room temperature owing to its unsuitable crystal packing. The yields are generally lower in solution and higher temperatures are required (**6**, 80 °C, 90%;[12] **8**, 80 °C, quantitative;[13] **10**, 25 °C, 88%;[14] **12**, 140 °C, 43%[15]). The present solid-state syntheses are a sustainable improvement and the need for separation and recovery of hydroquinone **4** is tolerable, as the products are insoluble in water. It is to be expected that numerous further syntheses will be successful with **2**, as the crystal structures of the various carbonyl partners do not seem to have much influence on the reactivity of the small and highly reactive hydrazine that escapes its cage for reaction in the ball-mill despite its six hydrogen bridges.

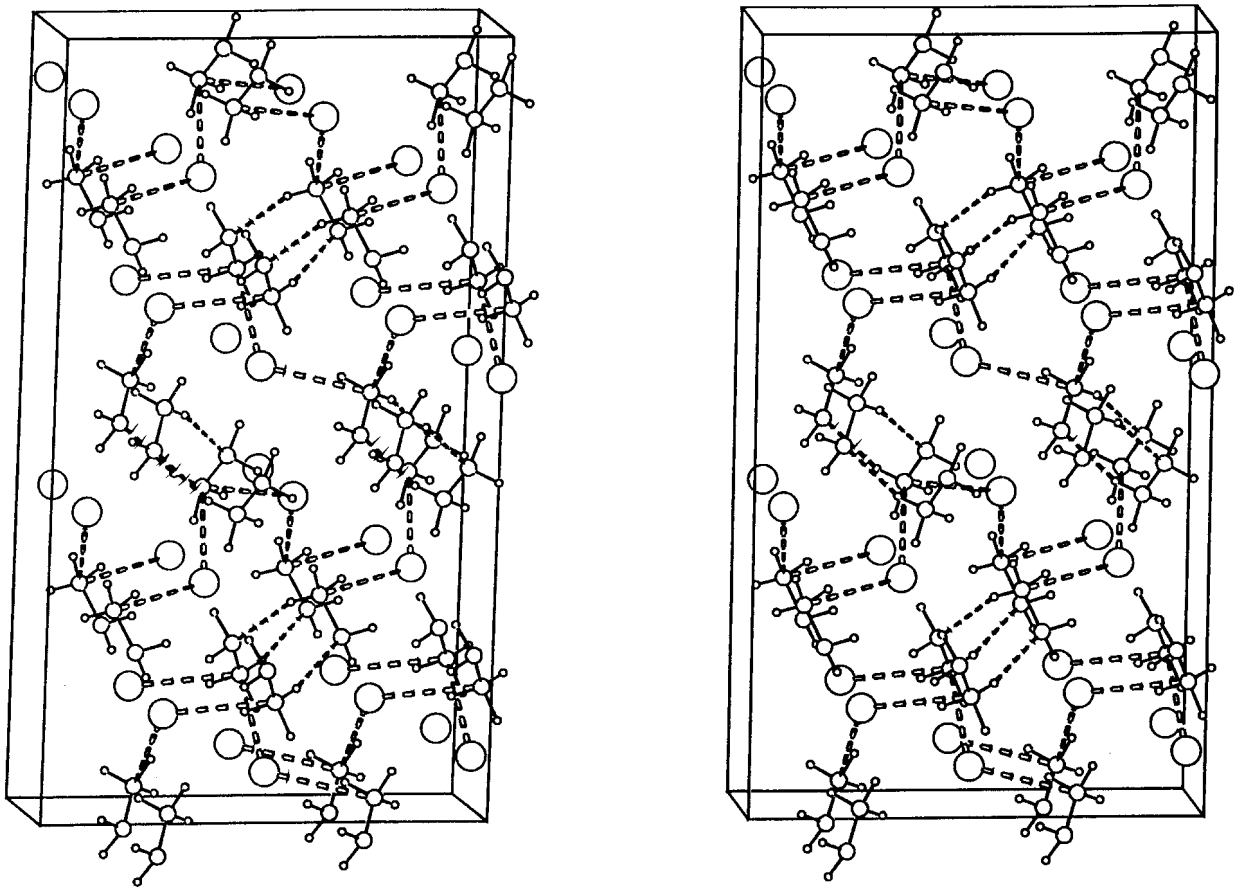

Figure 5. Stereoscopic view of the packing of $N_2H_4 \cdot HCl$ (rhombic, *Fdd*2)[11] skew on (001). Large circles are Cl, medium circles N and small circles H atoms; short ionic interactions ($Cl^- \cdots N^+$) and strong H-bridges are dotted; N—H$\cdots Cl^-$ bridges are not highlighted for clarity

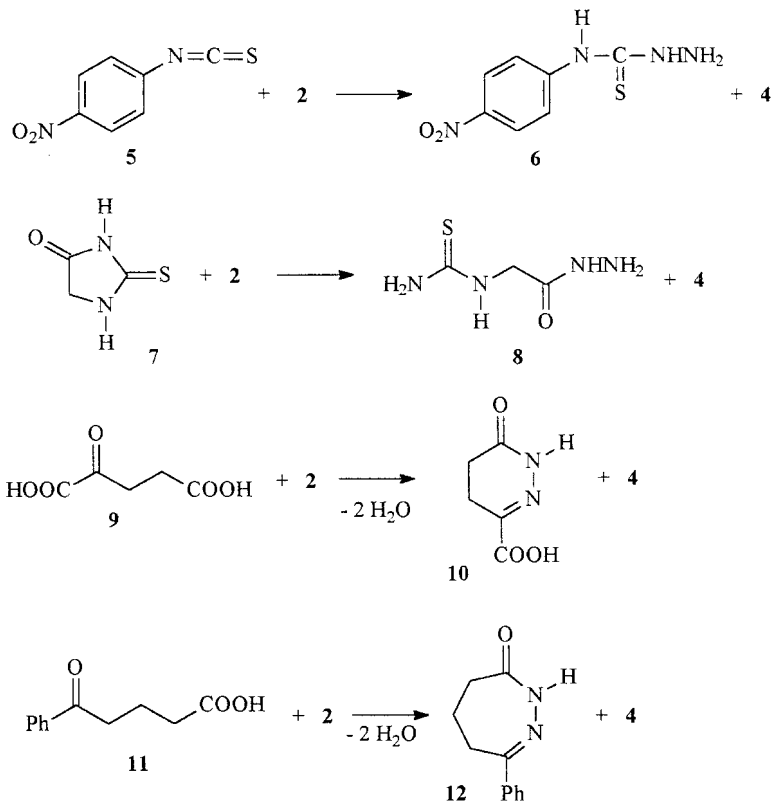

The reactions are not violent and it is likely that scale-ups in large mills can be easily controlled.

EXPERIMENTAL

Cantilever contact AFM with non-scraping[16] standard Si_3N_4 tips[8] at 10–30 nN force, the imaging techniques[8] and the possible tip–sample artifacts on rough surfaces[17] have been described. All AFM surface data are given in fully interactive VRML files at the epoc website at http://www.wiley.com/epoc.

Solid–solid techniques with AFM and ball-mills have been described.[2,8,10,18] A 4.00 mmol amount of the aldehyde/ketone **1** or 2.00 mmol of the (thio)carbonyl compound **5, 7, 9** or **11** were ball-milled with 2.00 mmol of **2** at 25–30 °C (70–80 °C in the case of **7**) for 1 h (3 h in the case of **1d**). The yields were quantitative in all cases. Spectroscopically pure (IR, ^{1}H- and ^{13}C NMR) mixtures of **4** (or its water clathrate) with the products **3, 6, 8, 10** or **12** were obtained. The previous host **4** was removed by 5 min of trituration with 20 ml of water, filtration and three washings with 2 ml of water each (at room temperature 10 ml of water dissolves 700 mg of **4** and 250 mg of **2**), the residue dried in a vacuum, weighed and again spectroscopically characterized.

The hydrazine–hydroquinone complex **2** was prepared according to Toda *et al.*[4] or obtained by recycling of the hydroquinone **4** from the aqueous washings of the reported solid-state syntheses (e.g. the reaction of **1a** and **2**) by evaporation, addition of 1.0 g of 80% hydrazine hydrate in water per 4.00 mmol of initially reacted **2** and recrystallization to give a 91% yield (520 mg) of spectroscopically pure **2**, m.p. 158 °C, after filtration, washing with water and drying.

*4-Hydroxybenzaldazine (**3a**).* Yield 98%; m.p. 270 °C (lit.[19] 270 °C); IR (KBr), 3338(OH), 1608 (C=N), 1592, 1515 cm^{-1}.

*4-Chlorobenzaldazine (**3b**).* Yield 99%; m.p. 207 °C (lit.[5] 208–210 °C).

*4-Dimethylaminobenzaldazine (**3c**).* Yield 99%; m.p. 273 °C (lit.[6] 274 °C).

*4-Nitroacetophenone azine (**3d**).* Yield 98%; m.p. 201 °C (lit.[7] 204 °C).

*4-(4-Nitrophenyl)thiosemicarbazide (**6**).* Yield 99%; m.p. 190 °C (lit.[12] 190 °C).

*Thiohydantoic acid hydrazide (**8**).* Yield 100%; m.p. 202 °C (lit.[13] 204 °C).

*6-Oxo-1,4,5,6-tetrahydropyridazine-3-carbonic acid (**10**).* Yield 98%; m.p. 194 °C (lit.[14] 194–195 °C).

*3-Phenyl-1,4,5,6-tetrahydro[1,2]diazepin-7-one (**12**).* Yield 99%; m.p. 156 °C (lit.[15] 157 °C).

EPOC material

The supplementary material available at the epoc website at http://www.wiley.com/epoc contains color images in GIF format and interactively usable full original 3D data of the images in VRML format in high and low resolution in order to allow for critical evaluation of the AFM results, their analytical use with suitable imaging software and future data mining. For example, the importance of unavoidable minor geometric artifacts at very steep features, that are not easily recognized in the common two-dimensional projections, can be judged in some of the three-dimensional views from various sides. However, it is safely concluded that these do not affect the conclusions derived from the stable scans (at least five consecutive scans) that also exclude nanoliquid phases in the reactions studied. The interactive analysis is possible with public domain software, e.g. Cosmo-Player or Blaxxun.

REFERENCES

1. Schmeyers J, Toda F, Boy J, Kaupp G. *J. Chem. Soc. Perkin Trans. 2* 1998; 989.
2. Kaupp G, Schmeyers J, Boy J. *Tetrahedron*, in press.
3. Kaupp G, Schmeyers J, Boy J. *Chemosphere* in press.
4. Toda F, Hyoda S, Okada K, Hirotsu K. *J. Chem. Soc., Chem. Commun.* 1995; 1531.
5. Mlochowski J, Giurg M. *Pol. J. Chem.* 1994; **68**: 2333.
6. Vickers S, Stuart EK. *Anal. Chem.* 1974; **46**: 138.
7. Miyatake K. *Yakugaku Zasshi* 1953; **73**: 455; *Chem. Abstr.* 1954; **48**: 5144.
8. Kaupp G. In *Comprehensive Supramolecular Chemistry*, vol. 8, Davies JED (ed). Elsevier: Oxford, 1996; 381–423 + 21 color plates; Kaupp G. *Chem. Unserer Zeit* 1997; **31**: 129; Engl. translation at http://kaupp.chemie.uni-oldenburg.de.
9. Kaupp G. *Mol. Cryst. Liq. Cryst.* 1992; **211**: 1.
10. Kaupp G, Boy J, Schmeyers J. *J. Prakt. Chem./Chem.-Ztg.* 1998; **340**: 346.
11. Chekhlov AN, Martynov IV. *Kristallografiya* 1988; **33**: 1010.
12. Lieber E, Ramachandran J. *Can. J. Chem.* 1959; **37**: 101.
13. Hideaki S, Tamatsu Y. *Yakugaku Zasshi*, 1967; **87**: 128; *Chem. Abstr.* 1967; **67**: 32379e.
14. Kline GB, Cox SH. *J. Org. Chem.* 1961; **26**: 1854.
15. Wermuth CG, König JJ. *Angew. Chem. Int. Ed. Engl.* 1972; **11**: 152.
16. Kaupp G. *Mol. Cryst. Liq. Cryst.* 1994; **252**: 259; Kaupp G. *J. Vac. Sci. Technol. B* 1994; **12**: 1952; Kaupp G, Plagmann M. *J. Photochem. Photobiol. A* 1994; **80**: 399.
17. Kaupp G, Herrmann A, Haak M. *J. Phys. Org. Chem.* 1999; **12**: 797.
18. Kaupp G, Schmeyers J, Kuse A, Atfeh A. *Angew. Chem., Int. Ed. Engl.* 1999; **38**: 2896.
19. Okafor EC. *Spectrochim. Acta, Part A* 1980; **36**: 207.